

LES OF FLOWS OVER SURFACES WITH CURVATURES

Siniša Krajnović

Chalmers University of Technology, Department of Applied Mechanics,
SE-412 96 Göteborg, Sweden
sinisa@chalmers.se

Abstract LES of flows around a three-dimensional hill and a finite cylinder mounted on a flat plate are presented. Inlet boundary conditions are made from a DNS results of low Reynolds number channel flow. Results are compared with existing experimental data.

INTRODUCTION

Many flows of engineering interest contain separations that occur on surfaces with curvatures. Such flows are more dependent on the viscous effects and upstream flow (inlet boundary conditions and boundary layer) than bluff body flows with sharp edge separation such as flow over a surface mounted cube or rectangular cylinder. This means that in LES of such a flow, the inlet boundary conditions must be similar to those in a real wind tunnel experiment and that the resolution of the upstream boundary layer becomes very important for the success of the simulation. These two requirements can be difficult to fulfill in LES of high Reynolds number flow.

In this paper we present LES of two flows, that around a three-dimensional hill and around a finite wall mounted cylinder. Both these flows contain separations on curved surfaces and are characterized with medium or high Reynolds numbers.

DESCRIPTION OF THE FLOWS AND NUMERICAL DETAILS

The three-dimensional hill used in the present work is that from the experiments by Simpson *et al* (1). The geometry of the body and the computational domain are given in Fig. 1. The geometry of the hill is defined by

$$\frac{y(r)}{H} = -\frac{1}{6.04844} \left[J_0(\Lambda) I_0 \left(\lambda \frac{r}{a} \right) - I_0(\Lambda) J_0 \left(\lambda \frac{r}{a} \right) \right]. \quad (1)$$

where $\Lambda = 3.1926$ and $a = 2H$ is the radius of the circular base of the hill. J_0 and I_0 are the Bessel function of the first kind and the modified Bessel function of the first kind, respectively. The Reynolds number, based on the maximum inlet velocity and

the hill height H is $Re = 1.3 \times 10^5$.

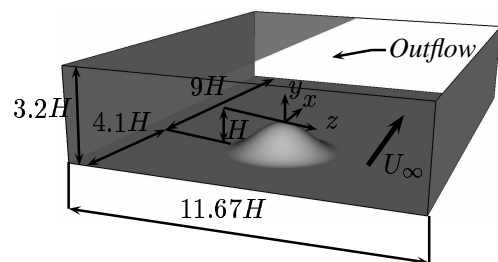


Figure 1: Computational domain with the axisymmetric hill.

The finite cylinder studied in this paper is that from the experiments by Park and Lee (2). A cylinder with an aspect ratio (L/D) of 6 was mounted vertically on a flat plate. Free stream inlet velocity $U_0 = 10 \text{ m/s}$ and diameter D equal with 0.03 m give a Reynolds number of approximately 20000.

A test section of $24D \times 20D \times 28D$ (width \times height \times length) was used in our simulation. The inlet and the outlet in our numerical wind tunnel are placed $8D$ and $19D$ from the cylinder, respectively.

Simulation of the hill is conducted using an orthogonal grid. It contains $256 \times 96 \times 192$ cells in x , y and z directions, respectively. A time step of $\Delta t U_{ref}/H = 0.0038$ is used. The averaging time, $t U_{ref}/H$, in the simulations is 103.8 (27,000 time steps).

For the cylinder flow simulation, a multi-block computational mesh was made. A grid topology was made using several O and C grids in order to concentrate most of the computational cells close to the cylinder. The large number of cells close to the surface is needed in order to resolve laminar boundary layer on the front part of the cylinder. Total of 7.1 million cells was used in the entire computational domain. Time step normalized with the inlet velocity U_0 and the cylinder diameter D was 0.00167. Maximum CFL number was smaller then one for all time steps.

Our LES simulations use the Smagorinsky subgrid scale model with van Driest damping function and the Smagorinsky constant of $C_s = 0.1$. LES equa-

tions are discretized using a 3D finite volume method for solving the incompressible Navier-Stokes equations using a collocated grid arrangement. Both convective and viscous plus sub-grid fluxes are approximated by central differences of second-order accuracy. The time integration is done using the second-order Crank-Nicolson scheme.

To simulate inlet velocity boundary condition in both simulations a separate direct numerical simulation of the channel flow with $Re_\tau = 500$ is conducted. Turbulence resulting from such low Reynolds simulation is of course different from that in our high Reynolds number channel. In order to fit the fluctuations from the channel flow to our new simulations, these are rescaled so that lower half of the channel (up to the center line) is scaled to boundary layer thicknesses δ_{99} in the hill and the cylinder flows, respectively. These fluctuations are superimposed to the boundary layer of the experimental mean profile. Besides the spatial fit, the temporal fit of the fluctuations from the channel flow was done.

RESULTS

Profiles for the velocities and the stresses from our LES of the hill flow were compared with the experimental data by Simpson *et al* (1) in the plane $x/H = 3.69$. The agreement of both the streamwise and the spanwise velocities is good (see Fig. 2). Some differences are observed in $\langle w \rangle_t / U_\infty$ velocity components above $y/H = 0.5$. Obviously there is secondary flow motion coming from the hill that is not represented in our LES. We found also that the Reynolds stresses were somewhat over-predicted in our simulation. However our results are in much better agreement with the experimental data than any in previous RANS simulations.

Our LES displayed instantaneous flow around cylinder with large number of small scale Kelvin-Helmholtz vortices (see Fig. 3a). Very thin horse-shoe vortex was observed at the junction of the cylinder with the plane. Surface pressure coefficients are compared with the experimental data by Park and Lee (2) in Fig. 3b. Similar to the experimental observations the separation point in our LES is more delayed closer to the free end (Fig. 3b). The agreement of $\langle C_p \rangle_t$ is better closer to the free end than at the half of the cylinder height. Thus LES does better job in the region with sharp edge separation than along the cylinder where prediction of the laminar boundary layer and transition are important. This indicates that finer resolution is required. Streamwise velocity and turbulence intensity are found to be under- and overpredicted, respectively, in our LES (not shown here). Finer meshes are constructed containing about 16 and 14 million nodes for the hill and the cylinder flow, respectively. These simulations are ongoing work and their results will be included in the

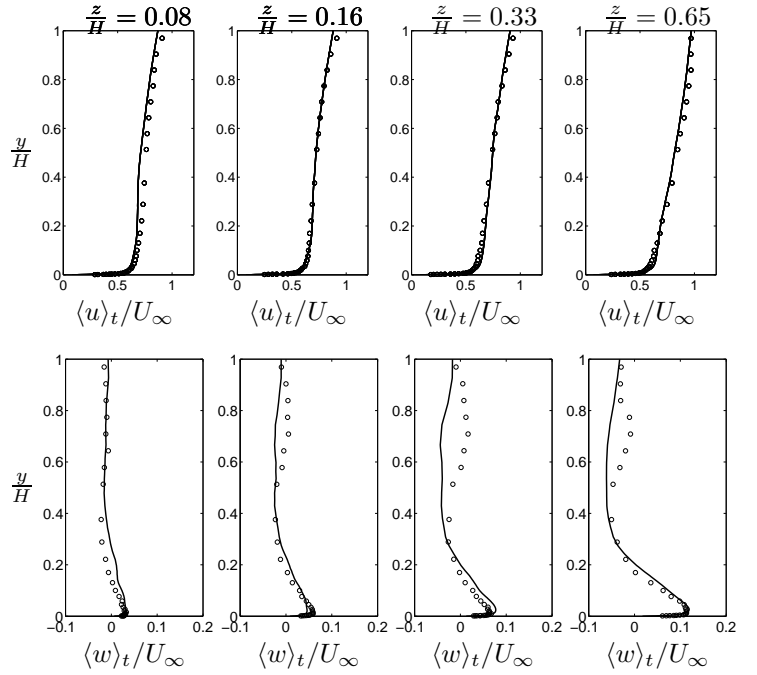


Figure 2: Hill flow. Streamwise $\langle u \rangle_t / U_\infty$ and spanwise $\langle w \rangle_t / U_\infty$ velocity components. Solid line: LES; markers: Experiments by Simpson *et al* (1).

presentation.

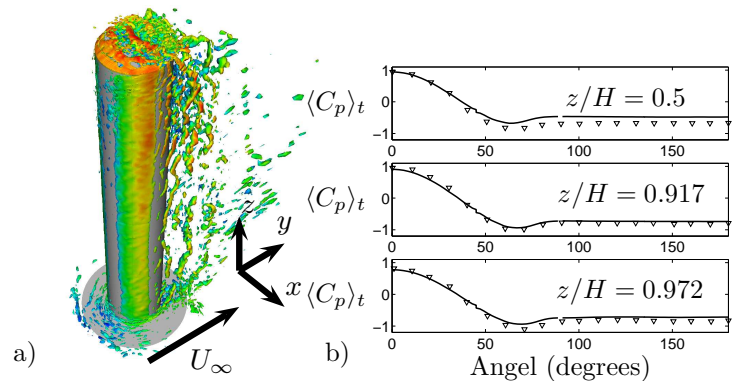


Figure 3: Cylinder flow. a) Instantaneous flow from LES. Second invariant of the velocity gradient $Q = 7000$ colored with the streamwise velocity. b) Surface pressure coefficient at three z locations. Solid line: LES; markers: Experiments by Park and Lee (2).

REFERENCES

- [1] Simpson, R. L. ; Long, C. H. ; Byun, G. (2002) Study of vortical separation from an axisymmetric hill. *Int. J. Heat and Fluid Flow* 23, pp. 582–591
- [2] Park, C-W. ; Lee, S-J. (2002) Flow structure around a finite circular cylinder embedded in various atmospheric boundary layers. *Fluid Dynamics Research* 30, pp. 197–215